General Equation for Size Nanocharacterization of the Core−Shell Nanoparticles by X-ray Photoelectron Spectroscopy

Jean-Numa Gillet* and Michel Meunier

Laser Processing Laboratory, Department of Engineering Physics, École Polytechnique de Montréal, C.P. 6079, succ. Centre-ville, Montréal, Québec H3C 3A7, Canada

Received: December 13, 2004; In Final Form: March 9, 2005

Nanocharacterization is essential for nanoengineering of new types of core−shell (c−s) nanoparticles, which can be used to design new devices for photonics, electronics, catalysis, medicine, etc. X-ray photoelectron spectroscopy (XPS) has been widely used to study the elemental composition of the c−s nanoparticles. However, the physical and chemical properties of a c−s nanoparticle dramatically depend on the sizes of its core and shell. We therefore propose a general equation for the XPS intensity of a c−s nanoparticle, which is based on an analytical model. With this equation, XPS can now also be used for nanocharacterization of the core and shell sizes of the c−s nanoparticles (with a diameter smaller than or equal to the XPS probing depth of ∼10 nm). To validate the new equation with experimental XPS data, we first determine the average shell thickness of a group of c−s nanoparticles by comparing the XPS intensity of reference bare cores to that of the c−s nanoparticles. Then we study the growth kinetics of the cores and shells of another group of c−s nanoparticles where the shells are obtained by oxidation.

I. Introduction

Core−shell (c−s) nanoparticles have recently generated an increasing interest owing to their promising technological applications in photonics, electronics, catalysis, medicine, etc.[1−14] Shell coating can be used to protect the nanoparticles from oxidation and improve their stability and compatibility in the surrounding milieu.[3−7,9,15−17] The shell can also be functionalized to bond the nanoparticle with nucleotides, proteins, other nanoparticles, etc.[4−7,9,16−18] However, the most spectacular feature of the c−s nanoparticles concerns their physical and chemical properties, which can significantly differ from those of the one-material (or individual) nanoparticles and can be engineered by varying their elemental composition as well as the sizes of their core and shell.[1−13,15−26] For instance, semiconducting c−s nanoparticles such as CdSe/ZnS (core/shell) can form quantum dots with a high photoluminescence quantum yield at room temperature, which is not possible with the individual CdSe nanoparticles, and a wavelength that is tunable from the blue to the red by changing the nanoparticle size.[6−8,15,16,19,20] Bimetallic and metallodielectric c−s nanoparticles such as Ag/Au and Au/SiO_2, respectively, can exhibit a surface plasmon band depending on the core and shell sizes.[17,22,25] Bimagnetic c−s nanoparticles such as FePt/Fe_3O_4 can generate an exchange coupling, which can be tuned by varying the sizes of the core and shell forming a magnetically hard and soft phase, respectively.[1−3,27] As a consequence, controlling the core and shell sizes is essential for nanoengineering of c−s nanoparticles with desired properties, which makes inevitable the need for developing new nanocharacterization methods.

X-ray photoelectron spectroscopy (XPS) has been widely used to determine the elemental composition of bulk materials near their surface[28,29] as well as those of thin films,[30,31] individual nanoparticles,[32−36] c−s nanoparticles,[21,31,37−41] etc. Measurement of the size of nanomaterials, such as the thickness of coating films thinner than ∼10 nm on a substrate, is another important XPS application.[30,31,42] Several authors were also able to determine the size of individual metallic nanoparticles from XPS studies.[34,35,43] On the other hand, XPS studies were performed to provide evidence of the c−s structure and shell growth for c−s nanoparticles of different types.[37−41]

In this paper, we demonstrate a general equation, which establishes an analytical relationship between the XPS intensity of a c−s nanoparticle and the sizes of its core and shell. Therefore, measurement of the core and shell sizes, which has been extensively performed by transmission electron microscopy (TEM), is now achievable by XPS for the c−s nanoparticles with a diameter of the order of the XPS probing depth of ∼10 nm or smaller than this value. Such c−s nanoparticles are the most promising for new technological applications since they can show particular quantum properties, which appear only below a critical size of few nm. With the new equation, the use of XPS shows a major advantage over other methods of nanocharacterization, such as TEM, since the sizes of the core and shell of the c−s nanoparticles and their elemental composition can all be obtained by XPS. As a first application of our equation, we determine the average shell thickness of a group of c−s nanoparticles by only measuring the XPS intensities of the coated and bare cores, independently of the atom densities and unattenuated intensities of the nanoparticle core and shell. This is possible for most types of c−s nanoparticles for which the XPS intensity of a reference bare core is measurable either before coating or after by removing the shell from the coated core, which can take a different radius than that of the bare core. Then, we study the growth kinetics of the core and oxide shell of metal-oxide and semiconductor-oxide c−s nanoparticles, which result from oxidation of initially bare cores, by measuring the XPS intensities of the nanoparticle core and shell at each subsequent oxidation time.

* Corresponding author. Phone: (+1)(514) 340-4711 ext. 7441. Fax: (+1)(514) 340-5195. E-mail: jngillet@videotron.ca.

10.1021/jp044322r CCC: $30.25
Published on Web 04/05/2005

SCHEME 1: Core−Shell (c−s) Nanoparticle with a Spherical Symmetry and Centered Core from Which the Photoelectrons with a normal Emission ($\psi_e = 0°$) Are Detected

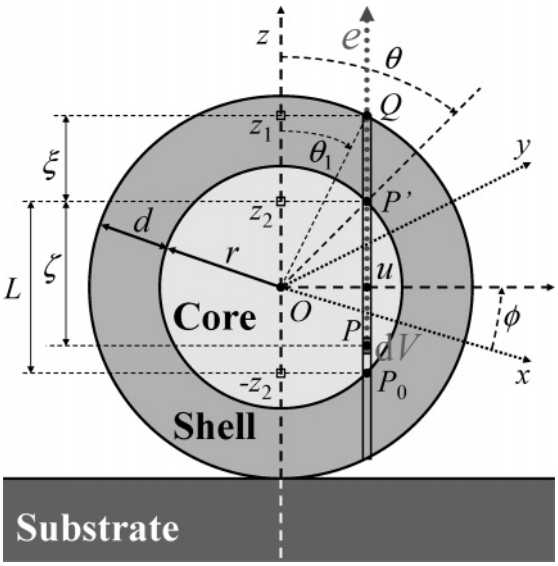

II. Theoretical Approach

To develop our model, we assume that the c−s nanoparticle has a spherical symmetry and centered core as in Scheme 1. This common assumption is a good approximation since the shell usually grows in a uniform manner around the core.[41] To compute the XPS signal intensity, we assume, as many authors,[30,35,41,43] an exponential intensity attenuation of the photoelectrons, which increases with the material thickness taken from one origin point *P*. Moreover, since the photoelectron detector is located very far from the c−s nanoparticles (compared to its diameter of few nm), we can consider only the parallel photoelectron rays emitted in only one direction, which is given by the *z* axis, for instance, in Scheme 1. Therefore, for a c−s nanoparticle, we can express the infinitesimal contribution d*I* of the photoelectrons, which are emitted in a given direction from a volume d*V* located at the core point *P*, to the XPS intensity *I* of the core as

$$\mathrm{d}I = I_0(E_Y)\exp\{-[\zeta/\lambda'(E_Y) + \xi/\lambda''(E_Y)]\}\,\mathrm{d}V \qquad (1)$$

where $I_0(E_Y)$ is the unattenuated intensity (per volume unit), which depends on the kinetic energy E_Y of the photoelectrons associated to a line *Y* in the XPS spectrum. In eq 1, $\zeta = |\mathbf{PP'}|$ and $\xi = |\mathbf{P'Q}|$ are the distances traveled by the photoelectrons inside the core and shell, respectively, as in Scheme 1. Equation 1 is different from the usual equation used for a one-material nanoparticle where $\xi = 0$ in the exponential argument.[43] In eq 1, $\lambda'(E_Y)$ and $\lambda''(E_Y)$, which only depend on E_Y, are the attenuation lengths (AL) of the photoelectrons in the core and the shell, respectively.

Because $\mathrm{d}V = \mathrm{d}\zeta\,\mathrm{d}A$ and the c−s nanoparticle can be entirely probed (owing to its diameter) by XPS, the core intensity *I* is obtained after triple integration in eq 1 over the core volume *V* as

$$I = \int\int_A J\,\mathrm{d}A \qquad \text{with } J = I_0\lambda'\exp(-c\xi/\lambda')[1 - \exp(L/\lambda')] \quad (2)$$

where the dependence of I_0 and λ' on E_Y is hidden for simplicity; and the surface intensity density *J* is obtained by integration over ζ that varies from 0 when $P = P'$ to a maximal distance of $L = |\mathbf{P_0P'}|$ when $P = P_0$, assuming a topology where the entire segment P_0P' is always inside the core as in Scheme 1. In eq 2, $c = \lambda'/\lambda''$ is the ratio of the AL in the core with respect to that in the shell. The AL was often believed to be identical to the inelastic mean free path (IMFP) of the photoelectrons,[30] which can vary by ±20% from one author to another[43] and is often unknown for the c−s nanoparticles.[41] Strong elastic-scattering effects are also expected for photoelectrons with low kinetic energies or materials with medium to high atomic numbers. As a consequence, the AL can significantly differ from the IMFP, so that an effective AL (EAL) must be used instead of the IMFP to evaluate the XPS intensity.[30,42] As other authors, we therefore propose to use the same EAL, λ, in the entire c−s nanoparticle for a given kinetic energy of the photoelectrons and a given relative abundance of the core atoms with respect to those of the shell.[41] Indeed, since the core and shell sizes are of the same order of magnitude than the λ-value being typically of ∼1 to 3 nm,[42] the EAL can reasonably be viewed in the entire c−s nanoparticle as being the same as that of an unstructured nanoparticle resulting from an alloy of the core and shell materials.[41] All further mathematical developments of eq 2 are also significantly simplified with this assumption, since we have $\lambda(E_Y) = \lambda'(E_Y) = \lambda''(E_Y)$ and, therefore, $c = 1$ in eq 2. On the other hand, *A* in eq 2 is the projected area resulting from the orthogonal projection of the core on a plane, which is perpendicular to all possible parallel trajectories of the core photoelectrons with the same takeoff angle ψ_e between a substrate normal and the *PQ* direction pointing to the photoelectron detector. In Scheme 1, $\psi_e = 0°$ owing to the *PQ* direction given by axis *z*. However, for a spherical c−s nanoparticle with a centered core, ξ and *L* in eq 2 are independent of ψ_e owing to the spherical symmetry, so that our calculations are valid for an arbitrary ψ_e assuming that no photoelectron trajectory intersects another neighboring nanoparticle when ψ_e is getting close to 90°. Consequently, a normal setup of the detector with respect to the substrate is not required to determine the XPS intensity *I*. Moreover $A = \pi r^2$ is given by the area of the disk resulting from the intersection of the equatorial plane *xOy* with the spherical core taking a radius *r*. In the Cartesian frame $\{O, x, y, z\}$, we have $\xi = z_1 - z_2$ and $L = 2z_2$, where z_1 and z_2 define the *z* coordinates of *Q* and *P'*, respectively, as in Scheme 1. In the spherical frame $\{O, r, \phi, \theta\}$, we can express z_2 and z_1 as a function of *r* as well as the shell thickness *d* and coazimuthal angles θ and θ_1 because $z_2 = r\cos\theta$ and $z_1 = (r + d)\cos\theta_1$. However, the vectors $\mathbf{OP'}$ and $\mathbf{OQ}$ defined in Scheme 1 have the same projection $u = r\sin\theta$ on the plane *xOy*, so that we have $\theta_1 = \arcsin[r\sin\theta/(r + d)]$, which depends on *r*, *d* and θ. Now we can express the surface element d*A* in eq 2 as $\mathrm{d}A = u\,\mathrm{d}u\,\mathrm{d}\phi = r^2\,\mathrm{d}\phi\sin\theta\cos\theta\,\mathrm{d}\theta$ because $\mathrm{d}u = r\cos\theta\,\mathrm{d}\theta$. After the variable change $\alpha = \cos\theta$, we obtain $\mathrm{d}A = -r^2\,\mathrm{d}\phi\,\alpha\,\mathrm{d}\alpha$. Therefore, *I* is obtained from eq 2 as a function of λ, *d*, and *r* as

$$I(\lambda,d,r) = nS(\lambda,r)F(d/\lambda,r/\lambda)$$
$$\text{with } F(\delta,\rho) = 2\int_0^1 \exp[-\gamma(\alpha,\delta,\rho)(\rho + \delta) + \alpha\,\rho][1 - \exp(-2\alpha\,\rho)]\,\alpha\,\mathrm{d}\alpha \quad (3)$$

where $\delta = d/\lambda$ and $\rho = r/\lambda$ are the dimensionless shell thickness and core radius, respectively, and $\gamma(\alpha,\delta,\rho) = \cos\{\arcsin[(1 - \alpha^2)^{1/2}\rho/(\rho + \delta)]\}$. Moreover *n* is the density of core atoms; and the atomic sensitivity factor is given by $S(\lambda, r) = I_0\lambda\pi r^2/n = j_0\sigma y_e U\lambda A$, where j_0 is the X-ray flux, σ is the cross section for the photoelectronic process, y_e is the quantum yield for the

photoelectron emission, and U is the instrument response function depending on E_Y.[36,39] The core intensity I in eq 3 results from the product of nS (which is equal to the XPS intensity of an uncoated bulk material with a top surface of projected area A and the same composition than that of the core) multiplied by a 2-D geometric factor $F(\delta, \rho)$, which is characteristic to the spherical geometry of the c−s nanoparticle. Moreover ϕ is integrated from $\phi = 0$ to $\phi = 2\pi$ in eq 3; and θ varies from 0 to $\pi/2$, so that α is integrated from $\alpha = 1$ to 0. For a c−s nanoparticle, there is no exact analytical solution for the integration over α in eq 3. However, in the particular case of an individual spherical nanoparticle, an exact analytical solution exists for eq 3. Indeed, when $d = 0$, we reobtain the preceding formula of refs 34 and 43 after integration by parts in eq 3, which gives the intensity $I(\lambda,d = 0,r)$ of the individual nanoparticle as

$$I(\lambda,d = 0,r) = nS(\lambda,r)F_1(r/\lambda) \text{ with } F_1(\rho) = 1 + [(2\rho + 1)e^{-2\rho} - 1]/(2\rho^2) \quad (4)$$

where $F_1(\rho)$ is the 1-D geometric factor of the individual nanoparticle. Nevertheless, when the core is much larger or much smaller than the shell, i.e., $r \gg d$ or $r \ll d$, respectively, we can obtain an analytical approximation of eq 3 as

$$I(\lambda,d,r) \approx nS(\lambda,r)F_1(r/\lambda)\exp(-d/\lambda) \quad (5)$$

Two important asymptotical cases can be derived from eq 5: First, if $r \gg \lambda$, we obtain from eq 5 a signal $I(\lambda, d, r)$ proportional to r^2 and find the same XPS signal, $I = nS\exp(-d/\lambda)$, than that (at normal emission) of a coated bulk material with a top surface of area A and coating film of thickness d.[30,31,42] In contrast to the preceding case, if $r \ll \lambda$, we calculate from eq 5 a signal, $I(\lambda, d, r)$, proportional to r^3, and obtain a signal, $I = NS\exp(-d/\lambda)/(\lambda A)$, that is proportional to the number $N = nV = n4\pi r^3/3$ of core atoms as noted in ref 34 for a small one-material nanocluster. However, for a c−s nanoparticle, the above asymptotical approximations of eq 3 do not hold, because d, r, and λ are of the same order of magnitude.

$I(\lambda, d, r)$ in eq 3 is computed by single instead of triple integration and can be numerically obtained with rapidity. We compute the integral $F(\delta, \rho)$ in eq 3, which is independent of λ, with a recursive adaptive Lobatto quadrature.[44] However, we can obtain after fitting of the numerical solution of $F(\delta, \rho)$ an approximate analytical equation of $I(\lambda, d, r)$. To find this equation, we first assume that the 2-D function $F(\delta, \rho)$ in eq 3 can be fitted as

$$F(\delta,\rho) \approx \exp(-\delta)h(\delta,\rho)F(\delta = 0,\rho) \text{ with } F(\delta = 0,\rho) = F_1(\rho) \quad (6)$$

where $h(\delta, \rho)$ is a 2-D transfer function and the analytic expression of the 1-D function $F_1(\rho)$ is obtained from eq 4. We now fit $h(\delta, \rho)$ in eq 6 with a trust-region algorithm[45] as

$$h(\delta,\rho) = [\kappa(\rho)\delta + 1]/(\delta + 1) \text{ with } \kappa(\rho) = (\beta_1\rho^2 + \beta_2\rho + 1)/(\beta_1\rho^2 + \beta_3\rho + 1) \quad (7)$$

In eq 7, $\kappa(\rho)$ is a 1-D fitting function, which is bounded as $0 \le \kappa(\rho) \le 1$ and tends to 1 when $\rho \ll 1$ or $\rho \gg 1$ to respect the asymptotical case in eq 5. Moreover we obtain by curve fitting the three constants: $\beta_1 = 0.002\,889\,84$, $\beta_2 = 0.051\,355\,94$, and $\beta_3 = 0.459\,824\,62$. These values result in a root-mean-square error between the numerical and analytical expressions of the geometric factor F, which is lower than 0.3% when $0 \le \delta \le 3$ and $0 \le \rho \le 6$. Consequently, from eqs 3, 6, and 7, we obtain a general analytical equation, with a low error, of the core intensity $I(\lambda, d, r)$ as

$$I(\lambda,d,r) = nS(\lambda,r)\exp(-d/\lambda)h(d/\lambda,r/\lambda)F_1(r/\lambda) \quad (8)$$

where $F_1(\rho)$ and $h(\delta, \rho)$ have analytical expressions given in eqs 4 and 7, respectively.

III. Applications and Results

Equation 8 gives a general relationship between the XPS signal intensity of a c−s nanoparticle and the sizes of its core and shell. However, I in eq 8 is an absolute intensity, which has to be compared with a reference to obtain a relative intensity that is independent of n and S. Indeed these quantities are usually not known for a c−s nanoparticle and S depends on the photoelectron detection system,[36,42] so that the absolute value of I in eq 8 cannot be used in practice. To obtain a relative intensity, we first consider the case of most types of c−s nanoparticles, where the XPS intensity I_b of a bare nanoparticle, with the same elemental composition as that of the core of the c−s nanoparticle to be analyzed, can be experimentally measured either before coating or after by removing the shell. In the XPS analysis of such a c−s nanoparticle, we use a spectral line Y resulting from a binding energy that is only representative of the core atoms. Hence only the core photoelectrons with the kinetic energy E_Y and EAL $\lambda_c = \lambda_c(E_Y)$ contribute to the intensity I_c of the coated core in the c−s nanoparticle. As I_b and I_c are given by eqs 4 and 8, respectively, we find a relative intensity I_b/I_c, which is independent of n and S. Therefore, by taking the natural logarithm of I_b/I_c, we obtain the following increasing 1-D function $i_c(\delta)$

$$i_c(\delta) = \ln(I_b/I_c) - \ln[\lambda_b{}^3G_b/(\lambda_c{}^3G_c)] = \delta + \epsilon_c(\delta,\rho_c) \text{ with } \epsilon_c(\delta,\rho) = \ln\{(\delta + 1)/[\kappa(\rho)\delta + 1]\} \quad (9)$$

from which the shell thickness d can be determined by XPS since $\delta = d/\lambda_c$. In eq 9, $\lambda_b = \lambda_b(E_Y)$ is the EAL of the photoelectrons from the reference bare cores; $\rho_b = r_b/\lambda_b$ and $\rho_c = r_c/\lambda_c$ are the predetermined average radii of the bare and coated cores, respectively, divided by their related EALs; and $\kappa(\rho)$ is the 1-D function in eq 7. Moreover, $G_b = \rho_b{}^2F_1(\rho_b)$ and $G_c = \rho_c{}^2F_1(\rho_c)$, which are both computed with eq 4, are the 1-D geometric factors of the bare and coated cores, respectively, which are multiplied by the square of their related normalized radius and takes different values for unequal ρ_b and ρ_c. As a consequence, eq 9 remains valid when the cores of the c−s nanoparticles have an average radius r_c that is different from that r_b of the reference bare cores, since ρ_b and ρ_c can have different values. In eq 9, $i_c(\delta)$ is formulated as a function of the natural logarithm of I_b/I_c, since we obtain the linear function $i_c(\delta) = \delta$ when $\rho_c \gg 1$ or $\rho_c \ll 1$, because $\kappa(\rho_c) = 1$, from eq 7, in these asymptotical cases of the coated bulk material or small atom cluster, respectively. However, as shown in Figure 1, a nonlinear correction term $\epsilon_c(\delta, \rho_c)$, which is computed for $\rho = \rho_c$ and bounded as $0 \le \epsilon_c \le \ln(\delta + 1)$, must be added to the asymptotical δ term of $i_c(\delta)$ in eq 9 for a c−s nanoparticle.

With eq 9, we determine by XPS the average shell thickness of a group of c−s nanoparticles with a gold core and polymeric shell made up of polypyrrole (PPy). Details of the experiments are given in ref 37. The XPS spectra in the Au 4f doublet region of the Au/PPy c−s nanoparticles and bare Au cores are shown by solid and dotted lines, respectively, in the Supporting Information (see Figure S1). The bare Au cores are obtained

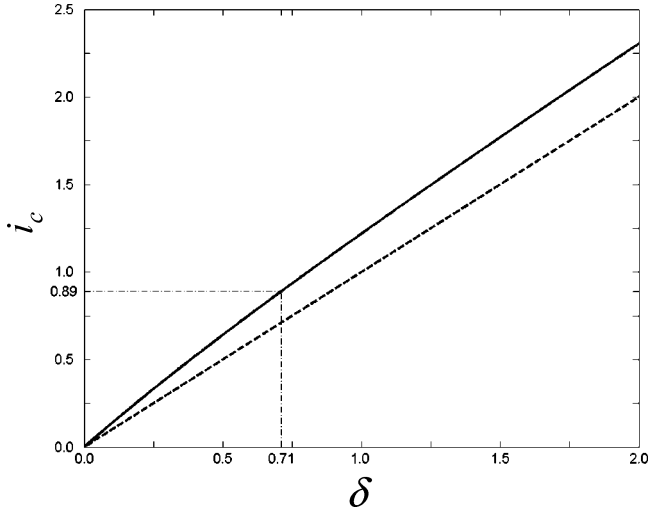

Figure 1. Curve of i_c vs δ (solid line) computed from eq 9 to determine the average shell thickness of Au/PPy c−s nanoparticles. The asymptotical case $i_c = \delta$ is shown by the dotted line.

from the Au/PPy c−s nanoparticles after shell removing.[37] From TEM images, one can also determine $r_b = 2.5$ nm and $r_c = 3.5$ nm.[37] By integration below both curves in Figure S1, which show no intensity offset, we compute $I_b/I_c = 1.12$, so that $i_c(\delta) = 0.892$ from eq 9. Moreover, we use the same value $\lambda_b = \lambda_c = 2$ nm for both EALs of the bare and coated Au cores than that of the mean free path proposed in ref 32 for the photoelectrons emitted from small Au nanoclusters in the Au 4f doublet region. Consequently, since $\delta = 0.714$ is computed from eq 9 or graphically from Figure 1, we obtain an average shell thickness of $d_{XPS} = 1.43$ nm. This value is in agreement with that obtained by TEM of $d_{TEM} = 1.50$ nm after averaging over 21 c−s nanoparticles.[37]

A second application of eq 8 is the XPS analysis of the growth kinetics of metal-oxide or semiconductor-oxide c−s nanoparticles with a shell obtained by surface oxidation of a bare core, such as Co/CoO, Ni/NiO, and Si/SiO_2 nanoparticles (see refs 2, 3, and 31, respectively). These types of c−s nanoparticles have recently gained a growing interest owing to their magnetic or optical properties but also because they can be fabricated with a gas-phase synthesis process in a clean system such as those used in semiconductor manufacturing in contrast to the usual processes of liquid-phase synthesis.[3] However, the simple formulation in eq 9 cannot be used in the complete XPS study of the growth kinetics of such a c−s nanoparticle. Indeed, if the c−s nanoparticle is fully oxidized, the coated-core intensity I_c is zero, which results in a singularity in eq 9. Consequently, to obtain a relative intensity that is usable to study the growth kinetics of such a c−s nanoparticle, we compare the shell intensity I_s to the addition of I_s and I_c. This ratio is equal to the relative concentration C_s of the valence atoms in the oxide shell, which are associated to the zerovalent atoms in the core, and is computed as

$$C_s(\lambda_0,\lambda_+,d) = I'_s/(\mu I'_c + I'_s) \text{ with } I'_c = I_c/I_{0c} \text{ and } I'_s = I_s/I_{0s} \quad (10)$$

where $\mu = n_0/n_+$ is the ratio of the density n_0 of the core atoms with respect to that n_+ of their corresponding valence atoms in the shell. In eq 10, $I_{0c} = n_0 j_0 \sigma y_e U$ and $I_{0s} = n_+ j_0 \sigma y_e U$ are the unattenuated intensities in the core and shell, respectively, where the instrument response functions U_0 and U_+ of the analyzed core and shell photoelectrons, respectively, approximately have the same value: $U \approx U_0 \approx U_+$. This approximation is

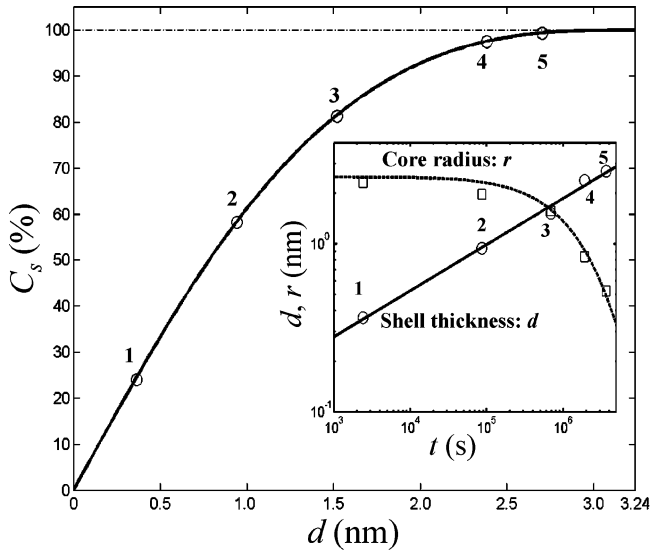

Figure 2. Curve of C_s vs d computed from eq 10 to determine the growth kinetics of Si/SiO_2 c−s nanoparticles; circles show XPS measurements of C_s for five oxidation times $t = t_1, t_2, ..., t_5$ (with $t_1 = 2.4 \times 10^3$ s and $t_5 = 3.63 \times 10^6$ s). Inset: log−log plots of d vs t (solid line) and r vs t (dotted line); circles and squares denote values of d and r, respectively, related to the experimental values of C_s.

reasonable assuming that the analyzed photoelectrons, which are emitted from the core and shell with the respective kinetic energies E_0 and E_+, are related to the same atomic orbital but for different valence species. Indeed the energy shift $|E_0 - E_+|$ in the XPS spectrum between the core and shell valence species may be of less than 1 eV to only ∼5 eV.[31−33,37] Moreover, in eq 10, $I_c = I(\lambda_0, d, r)$ and $I_s = I(\lambda_+, d = 0, r + d) - I(\lambda_+, d, r)$ are computed by using eq 8 with $\lambda_0 = \lambda(E_0)$ and $\lambda_+ = \lambda(E_+)$ being the EALs of the photoelectrons emitted from the core and the shell, respectively. Computation of C_s in eq 10 only requires the knowledge of the density ratio μ, because the normalized intensities I'_c and I'_s are independent of the absolute densities n_0 and n_+ as well as the XPS-process parameters j_0, σ, y_e, and U. Equation 10 also gives a relationship between C_s and the shell thickness d, noting that the core radius r is not an independent variable owing to another relationship between r and d, which is based on the conservation of the total number $N(t)$ of metallic or semiconducting atoms in the c−s nanoparticle. Indeed, at the oxidation time $t = 0$, we have $N(0) = n_0 4\pi r_0^3/3$ for the unoxidized core with a radius r_0. Then, at $t > 0$, an oxide shell with $d > 0$ grows on the core with a radius decreasing to $r < r_0$, so that $N(t) = n_0 4\pi r^3/3 + n_+ 4\pi[(r + d)^3 - r^3]/3$. However, the constraint $N(t) = N(0)$ must be fulfilled in the oxidized c−s nanoparticle, which results in the cubic-polynomial equation: $d_1^3 + 3r_1 d_1^2 + 3r_1^2 d_1 - \mu(1 - r_1^3) = 0$, where $r_1 = r/r_0$ and $d_1 = d/r_0$. By solving the latter equation for $r_1 = 0-1$ and keeping only the real root of d_1 for each r_1 value, we determine a relationship $r = r(d)$. Moreover, we find that the oxide-shell thickness d is bounded as $0 \le d \le \mu^{1/3} r_0$. Therefore, d can never exceed the value of $d_{max} = \mu^{1/3} r_0$.

With eq 10, we study the growth kinetics of Si/SiO_2 c−s nanoparticles on a HOPG substrate, which are oxidized in air. Details of the experiments are given in ref 31. At the oxidation time $t = 0$, the initial bare Si cores have an average radius $r_0 = 2.5$ nm. We use the EALs of $\lambda_0 = 3.0$ nm and $\lambda_+ = 3.5$ nm for the Si 2p photoelectrons emitted from the core and the shell, respectively. Assuming that the atom densities of Si and SiO_2 in a c−s nanoparticle are the same than those in bulk Si and SiO_2, we have $\mu = 2.185$ in eq 10. Thus, when the c−s nanoparticles are fully oxidized, their average shell thickness d

is maximal with a value of $d_{max} = \mu^{1/3} r_0 = 3.24$ nm. After insertion of the above data in eq 10, we obtain the numerical curve of C_s vs d, which is given by a solid line in Figure 2. Five experimental values of C_s related to five oxidation times from $t_1 = 2.4 \times 10^3$ s to $t_5 = 3.63 \times 10^6$ s were obtained by XPS measurements, as shown by circles in Figure 2. From these values and the numerical curve of C_s vs d, we extract five values of d corresponding to the oxidation times $t = t_1, t_2, ..., t_5$, which are shown by circles in the inset of Figure 2. By fitting the five points (d_k, t_k) for $k = 1, 2, ..., 5$, we obtain in a log−log plot a linear relationship of d vs t, which is drawn with a solid line in that inset. Moreover, since $r = r(d)$, we also compute the five corresponding values of r for $t = t_1, t_2, ..., t_5$, which are denoted by squares, and fit them with the dotted line in that inset. For the Si/SiO_2 nanoparticle, we therefore obtain the slope $\alpha_{ox} = 0.27$ for the curve of log d vs log t. As a consequence, the oxidation rate of a Si nanoparticles is lower than those of *c*-Si and *a*-Si bulk materials for which we previously obtained the slopes of $\alpha_{ox} = 0.61$ and $\alpha_{ox} = 0.72$ in log−log plots, respectively.[31]

IV. Conclusion

XPS nanocharacterization of the sizes of the core and shell of the c−s nanoparticles can now be achieved with a new equation. Indeed, this one establishes an analytical relationship between the XPS intensity of a c−s nanoparticle (with a diameter smaller than or equal to the XPS probing depth of ~10 nm) and the sizes of its core and shell. We showed two applications of the new equation: First, the average shell thickness of a group of c−s nanoparticles was determined independently of the core-and-shell atom densities. Then, we studied the growth kinetics of another group, which results from oxidation of bare cores.

Acknowledgment. We acknowledge J.-Y. Degorce for fruitful discussions, D.-Q. Yang and E. Sacher for their XPS experimental data, and the Natural Science and Engineering Research Council (NSERC) of Canada for its financial support.

Supporting Information Available: Experimental XPS-intensity spectra in the Au 4f doublet region for Au/PPy c−s nanoparticles (solid line) and bare Au cores (dotted line). XPS experimental data, taken from ref 37, to generate both curves without intensity offset are shown in Figure S1 by squares and circles for the Au/PPy and bare-Au nanoparticles, respectively. The experimental conditions to obtain both XPS spectra are assumed to be similar. This material is available free of charge via the Internet at http://pubs.acs.org.

References and Notes

(1) Zeng, H.; Li, J.; Wang, Z. L.; Liu, J. P.; Sun, S. *Nano Lett.* **2004**, *4*, 187.
(2) Skumryev, V.; Stoyanov, S.; Zhang, Y.; Hadjipanayis, G.; Givord, D.; Nogués, J. *Nature* **2003**, *423*, 850.
(3) Sakiyama, K.; Koga, K.; Seto, T.; Hirasawa, M.; Orii, T. *J. Phys. Chem. B* **2004**, *108*, 523.
(4) Vestal, C. R.; Zhang, Z. J. *J. Am. Chem. Soc.* **2002**, *124*, 14312.
(5) Lyon, J. L.; Fleming, D. A.; Stone, M. B.; Schiffer, P.; Williams, M. E. *Nano Lett.* **2004**, *4*, 719.
(6) Wargnier, R.; Baranov, A. V.; Maslov, V. G.; Stsiapura, V.; Artemyev, M.; Pluot, M.; Sukhanova, A.; Nabiev, I. *Nano Lett.* **2004**, *4*, 451.
(7) Wang, D.; He, J.; Rosenzweig, N.; Rosenzweig, Z. *Nano Lett.* **2004**, *4*, 409.
(8) Kim, S.; Fisher, B.; Eisler, H.-J.; Bawendi, M. *J. Am. Chem. Soc.* **2003**, *125*, 11466.
(9) Lu, Y.; McLellan, J.; Xia, Y. *Langmuir* **2004**, *20*, 3464.
(10) Kamata, K.; Lu, Y.; Xia, Y. *J. Am. Chem. Soc.* **2003**, *125*, 2384.
(11) Riley, T.; Heald, C. R.; Stolnik, S.; Garnett, M. C.; Illum, L.; Davis, S. S. *Langmuir* **2003**, *19*, 8428.
(12) Harpeness, R.; Gedanken, A. *Langmuir* **2004**, *20*, 3431.
(13) Park, N.-G.; Kang, M. G.; Kim, K. M.; Ryu, K. S.; Chang, S. H. *Langmuir* **2004**, *20*, 4246.
(14) Mandal, S.; Selvakannan, P.; Pasricha, R.; Sastry, M. *J. Am. Chem. Soc.* **2003**, *125*, 8440.
(15) Kilmov, V. I.; Mikhailovski, A. A.; Xu, S.; Malko, A.; Hollingsworth, J. A.; Leatherdale, C. A.; Eisler, H.-J.; Bawendi, M. G. *Science* **2000**, *290*, 314.
(16) Chan, W. C. W.; Nie, S. *Science* **1998**, *281*, 2016.
(17) Cao, Y. W.; Jin, R.; Mirkin, C. A. *J. Am. Chem. Soc.* **2001**, *123*, 7961.
(18) Wang, Y.; Teng, X.; Wang, J.-S.; Yang, H. *Nano Lett.* **2003**, *3*, 789.
(19) Cherniavskaya, O.; Chen, L.; Islam, M. A.; Brus, L. *Nano Lett.* **2003**, *3*, 497.
(20) Alivisatos, A. P. *Science* **1996**, *271*, 933.
(21) Teng, X.; Black, D.; Watkins, N. J.; Gao, Y.; Yang, H. *Nano Lett.* **2003**, *3*, 261.
(22) Lu, Y.; Yin, Y.; Li, Z.-H.; Xia, Y. *Nano Lett.* **2002**, *2*, 785.
(23) Jiang, P.; Bertone, J. F.; Colvin, V. L. *Science* **2001**, *291*, 453.
(24) Liang, Z.; Susha, A.; Caruso, F. *Chem. Matter.* **2003**, *15*, 3176.
(25) Graf, C.; v. Blaaderen, A. *Langmuir* **2002**, *18*, 524.
(26) Breen, M. L.; Dinsmore, A. D.; Pink, R. H.; Qadri, S. B.; Ratna, B. R. *Langmuir* **2001**, *17*, 903.
(27) Zeng, H.; Li, J.; Liu, J. P.; Wang, Z. L.; Sun, S. *Nature* **2002**, *420*, 395.
(28) Wagner, C. D.; Riggs, W. M.; Davis, L. E.; Moulder, J. F.; Muilenberg, G. E. *Handbook of X-ray Photoelectron Spectroscopy*; Perkin-Elmer: Eden Prairie, MN, 1978.
(29) Tilinin, I. S.; Jablonski, A.; Tougaard, S. *Phys. Rev. B* **1995**, *52*, 5935.
(30) Jablonski, A.; Powell, C. J. *J. Alloy Compd.* **2004**, *362*, 26.
(31) Yang, D.-Q.; Gillet, J.-N.; Meunier, M.; Sacher, E. *J. Appl. Phys.* **2005**, *97*, 024303.
(32) Boyen, H.-G.; Kästle, G.; Weigl, F.; Koslowski, B.; Dietrich, C.; Ziemann, P.; Spatz, J. P.; Riethmüller, S.; Hartmann, C.; Möller, M.; Schmid, G.; Garnier, M. G.; Oelhafen, P. *Science* **2002**, *297*, 1533.
(33) Koslowski, B.; Boyen, H.-G.; Wilderotter, C.; Kästle, G.; Ziemann, P.; Wahrenberg, R.; Oelhafen, P. *Surf. Sci.* **2001**, *475*, 1.
(34) Werthein, G. K.; DiCenzo, S. B. *Phys. Rev. B* **1988**, *37*, 844.
(35) Piyakis, K. N.; Yang, D.-Q.; Sacher, E. *Surf. Sci.* **2003**, *536*, 139.
(36) Katari, J. E. B.; Colvin, V. L.; Alivisatos, A. P. *J. Phys. Chem.* **1994**, *98*, 4109.
(37) Liu, Y.-C.; Chuang, T. C. *J. Phys. Chem. B* **2003**, *107*, 12383.
(38) Liu, S.; Ma, Y.; Armes, S. P.; Perruchot, C.; Watts, J. F. *Langmuir* **2002**, *18*, 7780.
(39) Cao, Y. W.; Banin, U. *J. Am. Chem. Soc.* **2000**, *122*, 9692.
(40) Dabbousi, B. O.; Rodriguez-Viejo, J.; Mikulec, F. V.; Heine, J. R.; Mattoussi, H.; Ober, R.; Jensen, K. F.; Bawendi, M. G. *J. Phys. Chem. B* **1997**, *101*, 9463.
(41) Hoener, C. F.; Allan, K. A.; Bard, A. J.; Campion, A.; Fox, M. A.; Mallouk, T. E.; Webber, S. E.; White, J. M. *J. Phys. Chem.* **1992**, *96*, 3812.
(42) Jablonski, A.; Powell, C. J. *Surf. Sci.* **2002**, *520*, 78.
(43) Lörinčík, L. *Appl. Surf. Sci.* **1992**, *62*, 89.
(44) Gander, W.; Gautschi, W. *BIT* **2000**, *40*, 84.
(45) Branch, M. A.; Coleman, T. F.; Li, Y. *SIAM J. Sci. Comput.* **1999**, *21*, 1.